International Journal of Architectural, Civil and Construction Sciences
ISSN: 2415-1734
Vol:11, No:5, 2017

# Finite Element Modeling for Clamping Stresses Developed in Hot-Driven Steel Structural Riveted Connections

Jackeline Kafie-Martinez, Peter B. Keating

***Abstract*—**A three-dimensional finite element model is developed to capture the stress field generated in connected plates during the installation of hot-driven rivets. Clamping stress is generated when a steel rivet heated to approximately 1000 °C comes in contact with the material to be fastened at ambient temperature. As the rivet cools, thermal contraction subjects the rivet into tensile stress, while the material being fastened is subjected to compressive stress. Model characteristics and assumptions, as well as steel properties variation with respect to temperature are discussed. The thermal stresses developed around the rivet hole are assessed and reported. Results from the analysis are utilized to detect possible regions for fatigue crack propagation under cyclic loads.

***Keywords*—**Clamping stress, fatigue, finite elements, rivet, riveted railroad bridges.

## I. Introduction

OLDER railroad bridges currently in service in North America are riveted structures that were built near the beginning of the 20th century. These bridges are now being subjected to much higher live loads than what they were originally designed for [1]. The passage of many trains per day subjects the mechanical fasteners into an array of variable amplitude stresses, which ultimately affects the fatigue life of the structure.

An accurate estimation of the fatigue life of riveted steel structural connections is very much needed. It has been observed that cracks usually emanate from the edge of a rivet hole, since rivet holes are the major locations of stress concentration. The riveting process itself causes significant residual stresses around the rivet hole.

Riveting is a method of joining together structural components by inserting a metal pin, called a rivet, into a matching hole previously done on the jointed pieces. At installation, the rivet consists of a shank and a head, known as *manufactured head*. The rivet is heated to approximately 1000 °C before inserting it into the holes in order to forge a second head, known as *driven head*, and in this way permanently fastened the plies or layers of plate. Riveting is essentially a forging process. As the rivet cools, it thermally contracts, subjecting the material being fastened into a compressive stress.

Early studies have shown that rivets can develop clamping stresses approximately equivalent to the yield strength of rivets [2].

Studies have demonstrated that clamping force is a principal variable influencing the fatigue resistance of riveted connections typical in old railroad bridges [3]. Rivet clamping stress enhances the fatigue strength by introducing a localized compression field, retarding the process of crack formation or propagation. However, clamping stress is hard to quantify, and if measured experimentally, it has been reported that it varies widely; thus, it is not usually accounted for in a fatigue life analysis.

Zhou [4] conducted a study to measure the magnitude of clamping residual stress in riveted members from demolished bridges approximately 60 years of age. The measured clamping stress varied from 34 to 165 MPa (5 to 24 ksi), with an average of about 83 MPa (12 ksi) and a standard deviation of about 41 MPa (6 ksi). Zhou [4] also performed a two-dimensional finite element model to examine the distribution of normal and frictional stresses on the contact surfaces. The presence of a crack was not considered in the model. It was reported that a temperature change of 204 °C (400 °F) during the cooling process in the rivet caused a clamping stress of about 262 MPa (38 ksi).

Al-Bahkali [5] developed a three-dimensional finite element model for lap riveted and rivet-bonded joints. A heat transfer analysis was performed to simulate the thermal stresses induced when the hot rivet transfers heat to the environment by convection. The analysis was proceeded by an elastic analysis where one of the plates is subjected to a constant velocity to simulate a lap shear tensile test up to failure. It was concluded that introducing an adhesive layer between the connecting plates vastly reduces the stresses developed in the joints, decreases stress concentrations, and increases fatigue life.

De Jesus et al. [6] performed a finite element model of riveted and bolted joints made of puddle iron to study the crack initiation and propagation phases in these kinds of connections. A finite element model using solid and contact elements was performed; clamping stresses as well as friction were considered. Finally, a through thickness crack depth was modeled, and the stress intensity factor was obtained for several crack lengths using the Virtual Crack Closure Technique (VCCT).

In summary, while several finite element analyses have been performed, most of these studies have been carried out in extremely thin plates (mostly used for aircraft structures), and

J. Kafie (PhD candidate) and P. B. Keating (Associate Professor) are with the Civil Engineering Department at Texas A&M University, College Station, TX 77843 USA (e-mail: jackeline_01@ tamu.edu, keating@civil.tamu.edu).

typically the residual stresses alone were not reported. These residual stresses are extremely important for future analyses since their inclusion replicates more realistically the initial condition of the riveted plates before any mechanical loading begins affecting fatigue life. Motivated by the need for greater understanding of the rivet clamping stress field, a three-dimensional finite element model was developed to capture the stress field around the rivet hole.

## II. Computer Simulation: Finite Element Model

### A. Geometry

The configuration chosen for the model consisted of two axially loaded steel plates, each 15.9 mm (5/8 inches) thick by 152.4 mm (6 inches) wide, joined at their centers by a steel structural rivet with a diameter of 22.2 mm (7/8 inches). This simulates a bottom flange of a built-up plate girder.

The length of the plate was chosen to be large enough so that it would have a negligible effect on the analysis at the rivet. It was also assumed a null clearance between the rivet and the hole. The three-dimensional finite element model was developed using ABAQUS© software.

The main purpose of the model is to capture the residual stress field generated during the installation of hot-driven rivets. In other words, the stresses induced in the plates by the thermal contraction of the rivet as it cools. This makes the analysis a thermal analysis, and the resulting residual stresses, thermal stresses. It was necessary to define a coupled temperature-displacement step. This type of analysis is a fully coupled, simultaneous heat transfer and stress analysis, where the simultaneous solution of the temperature and stress/ displacement fields is necessary.

### B. Material Properties

The material's properties necessary to perform this kind of analysis are: conductivity, specific heat capacity, volumetric thermal expansion, density, Poisson's ratio, and Young's modulus [7]. Except for the material's density and thermal expansion, the dependence of the material properties with respect to temperature was considered [8]. Moreover, the interfacial gap conductance was necessary to specify the heat transfer between steel- air- steel interfaces.

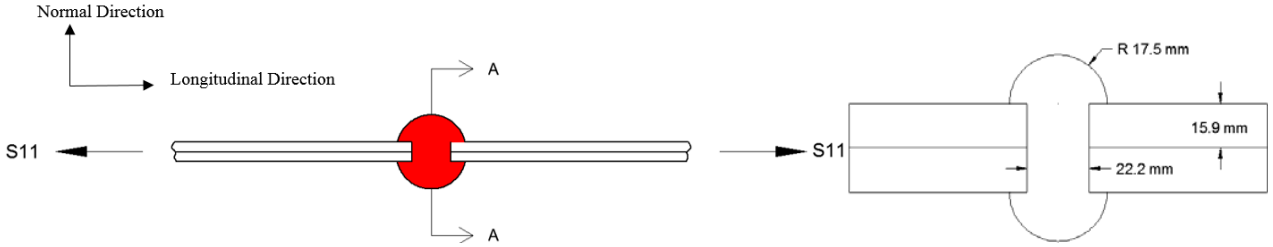


(a) (b) Section A-A

Fig. 1 Two steel plates riveted at midspan (a) Longitudinal view (b) Transverse view

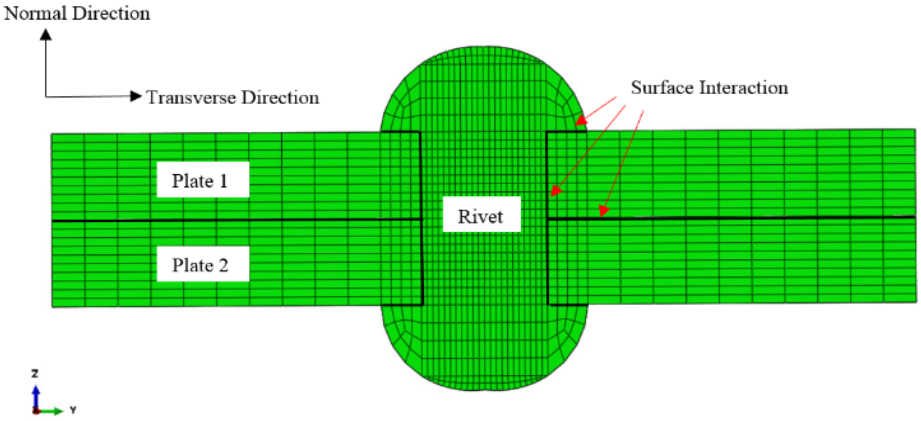


Fig. 2 Riveted model fine mesh in critical area

### C. Mesh/Element Type

All components were modeled using an 8-node thermo-mechanically-coupled brick, trilinear displacement and temperature, reduced integration elements (C3D8RHT).

The rivet consisted of 17,120 elements, and each plate consists of 59,920 elements. The model requires a very fine mesh in the vicinity of the rivet hole, which is the area of the plate right under the rivet head and throughout the thickness. To study the thermal stress for various thickness, a number of elements were considered.

### D. Predefined Fields

The initial temperature of the rivet was assumed to be 1000

°C, and the plates were assumed to be at ambient temperature. In order to define the initial temperature fields in ABAQUS, it was necessary to create a predefined field for the plate and for the rivet. The predefined fields state the initial condition of the plate and of the rivet.

### *E. Boundary Conditions*

Boundary conditions are necessary to guarantee convergence. The plates were considered to be simply supported. Moreover, a temperature boundary condition was defined to terminate the analysis when thermal equilibrium (ambient temperature) of the entire system has been reached.

### *F. Interactions/Contact Elements*

All the contact surfaces have a coefficient of friction of 0.3 (tangential behavior), overclosure hard contact surface (normal behavior) and interfacial gap conductance. The master surfaces were set on the plates, and the slave surfaces were set on the rivet. The *Nlgeom* option must be enabled to account for large strain plastic deformations.

## III. Results and Discussion

The complexity of the model increases significantly with the usage of contact surface interactions. Difficulty in making the analysis converge is a very common issue in contact analyses.

ABAQUS documentation suggests loading the system in small increments by reducing the increment size in the *Step* dialog box. After several iterations, it was found that the model converged nicely when the initial increment size was set to 0.001, with a minimum of $1x10^{-6}$ and a maximum of 0.01. However, when the study was performed using thinner plates, these small increments alone were not sufficient to make the solution converge. To perform a parametric study of the effect of plate thickness in the residual stress field and to be unanimous between all the finite element models, the *Automatic Stabilization* option, within the step definition and presented in the step dialog box, was used with default values for dissipated energy fraction and maximum ratio of stabilization to strain energy, 0.002 and 0.05, respectively. If automatic stabilization is used, it is necessary to check the history output if the energy dissipated by viscous damping is less than 5% of the internal strain energy (defined as ALLSD and ALLIE, respectively, on ABAQUS). If it is less than 5%, it can be assumed that the accuracy was not significantly affected by automatic stabilization. It is important to note that not always the default value is adequate, therefore obtaining the optimal value for the damping factor is a trial and error process until a converged solution is obtained and the dissipated stabilization energy is sufficiently small.

### *A. Deformation and Stress Contours*

The usage of overclosure hard contact surfaces prevented the contacting surfaces from penetrating one another; it also allows them to separate and loose contact as needed. Therefore, the use of contact surfaces gives a realistic deformed shape.

For the model to be correct, the deformation behavior should exhibit the following characteristics:

1. The rivet head will shrink in size.
2. As the rivet contracts, the plates will try to squeeze out; this will be reflected as a gap between the rivet shank and the plate.
3. As the rivet cools, the area near the rivet hole is compressed, however far away from this area the plates will tend to separate.

Fig. 3 shows the deformed and undeformed shape of the riveted plate seen in transverse view. Note that in the deformed shape, the rivet head has shrunk, and there is a gap between the rivet shank and the plates. Fig. 4 shows the separation of the plates in its transverse view.

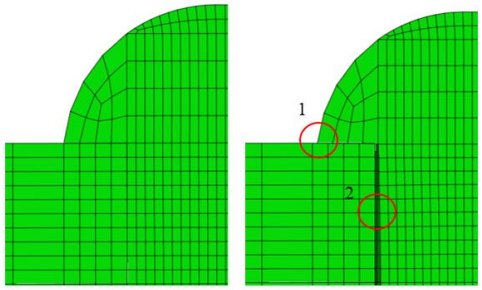


Fig. 3 (a) undeformed and (b) deformed shape. The rivet head will shrink and the plates will try to squeeze themselves out as the rivet compress

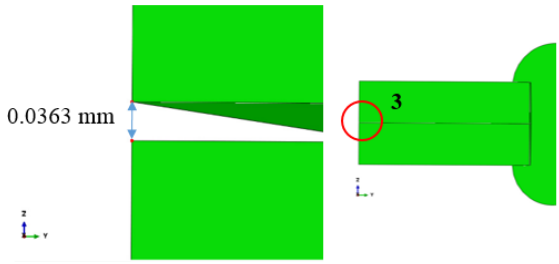


Fig. 4 Separation of the plates far away from the rivet hole (transverse view)

The results of the analysis are shown in Fig. 5. Thermal stress contours are shown for the Von Mises stress criteria, normal and longitudinal stress (S33 and S11, respectively). The normal stress, S33, normal to the longitudinal axis of the rivet, is the clamping stress. Note from the stress contour that both plates are under compression underneath the rivet head, while the rivet shank is subjected to tensile stress. The compression stress right under the rivet head adds up to 303 MPa (44 ksi). Zhou [4] reported a clamping stress of 262 MPa (38 ksi) in the axial direction of the rivet shank for a temperature differential of 205 °C (400 °F).

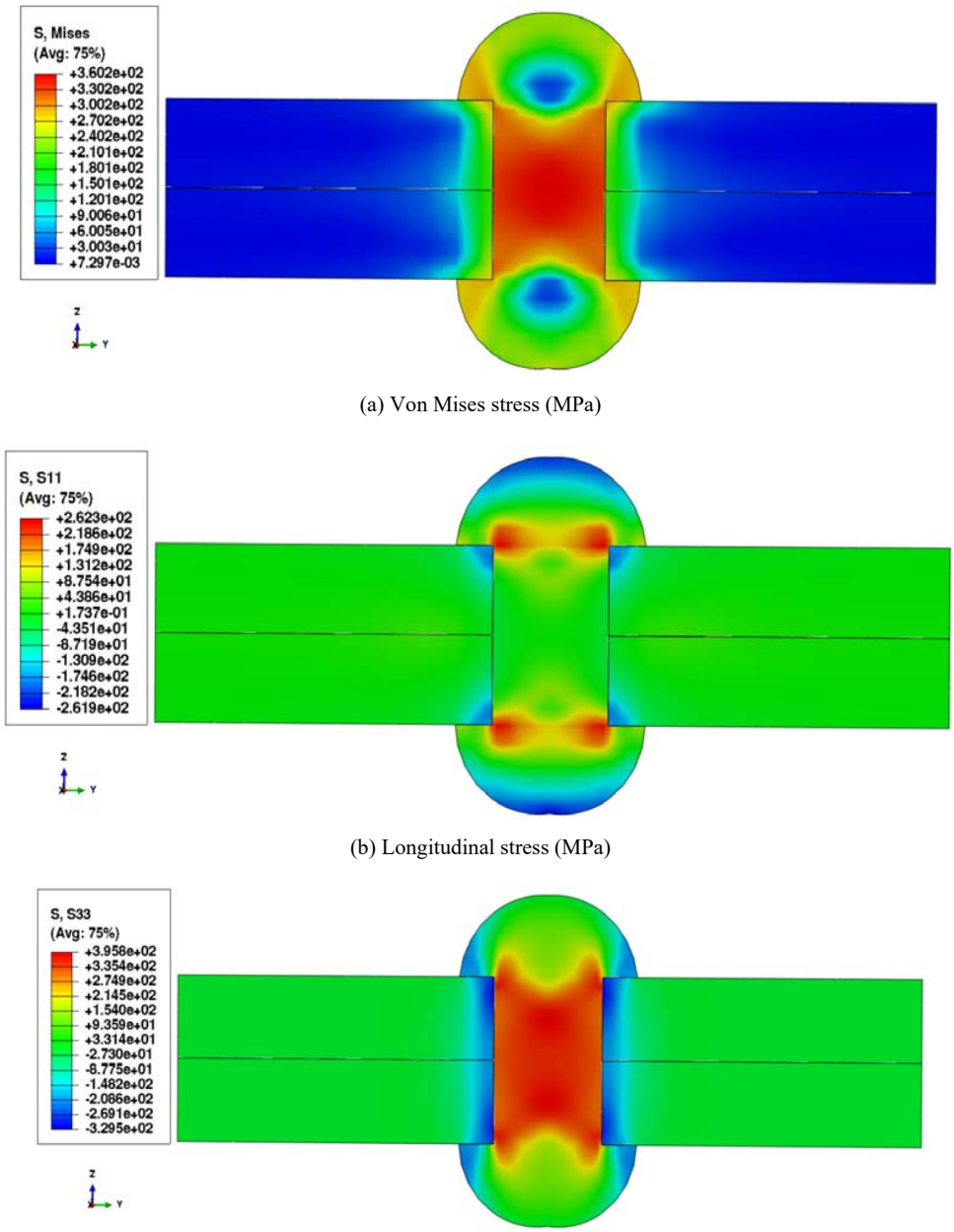


(a) Von Mises stress (MPa)

(b) Longitudinal stress (MPa)

(c) Clamping stress (MPa)

Fig. 5 Thermal stress contours for the riveted model (a) Von Mises stress (b) Longitudinal stress (c) Normal stress (clamping stress). Positive stress is tension

### *B. Effect of Plate Thickness on Clamping Stresses*

Thicker elements generally have a lower fatigue strength than thinner elements [9]. Therefore, the magnitude of the clamping stress might be dependent on the thickness of the material being fastened. In order to perform a parametric study of the effect of plate thickness in the generation of residual stresses, the finite element analysis was performed numerous times assuming different plates thicknesses. Five models were done with the following plates' thicknesses: 3.18 mm (1/8 in), 6.35 mm (1/4 in), 7.94 mm (5/16 in), 12.7 mm (1/2 in), and 15.9 mm (5/8 in).

The normal through-thickness (S33) and longitudinal (S11) stresses were obtained in the following way: for each of the models, ten elements were used throughout the plate thickness. Stresses were recorded in these ten elements at the edge of the rivet hole and perpendicular to the longitudinal axis of the plates. Figs. 6 and 7 show the normal and longitudinal stresses of the five riveted plates. The plate thickness of zero, is located in the plate, under the rivet head at the hole perimeter.

In the five cases, the plates were under compressive stress in the area underneath the rivet head and throughout the thickness. However, as the plate thickness increases, the magnitude of the stress between faying surfaces lowers significantly. From Fig. 6, the thickest plate (15.9 mm) has the highest compressive stress under the rivet head, however it has the least compressive stress between faying surfaces. Moreover, Fig. 7 clearly shows how the compressive stress decreases with increasing plate thickness. This is relevant since it will most likely dictate the possible location for future fatigue cracks. Furthermore, it is generally accepted that compressive residual stresses reduces the fatigue crack growth rate, and tensile stresses increases it [10]. Therefore, thinner plates will exhibit slower fatigue crack growth rate and a higher residual stress effect.

### *C. Possible Regions of Crack Propagation*

Clamping stress is a permanent residual stress that will present itself during the riveting process. That rivet is part of a structural connection that will most likely experience live loads. This analysis is extended by subjecting the riveted plates into a mechanical tensile traction to determine how the two types of stresses (thermal and mechanical) developed. Assuming no shear transfer between plates, but instead, the component is located in a constant moment region, a 65 MPa (9.42 ksi) was applied to both plates. This tensile stress was obtained by assuming a train consisting of three locomotives (SD70) and 110 railcars (each weighing 157.5 tons or 315,000 pounds) [11].

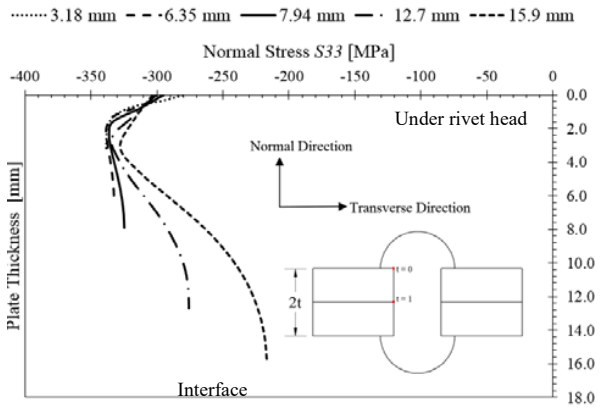


Fig. 6 Clamping stress field variation throughout the plate thickness for different plate thicknesses

The solid line of Fig. 9 represents the stress field due to thermal and mechanical stress (65 MPa). Crack propagation due to a longitudinal tensile stress will generate a crack perpendicular to the stress and emanating from the rivet hole, as shown in Fig. 8. In the case of thin plates, the crack would most likely be a through thickness crack. However, if the plate is of considerable thickness, the crack could start either underneath the rivet head or, under the rivet head and between faying surfaces. Fig. 9 describes how the clamping stress changes from compressive to tensile. Since tensile stress is responsible for crack propagation, it is likely that the crack will form between faying surfaces.

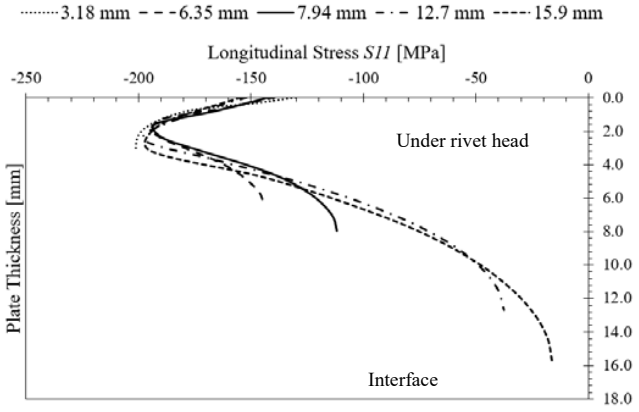


Fig. 7 Longitudinal residual stress field variation throughout the plate thickness for different plate thicknesses

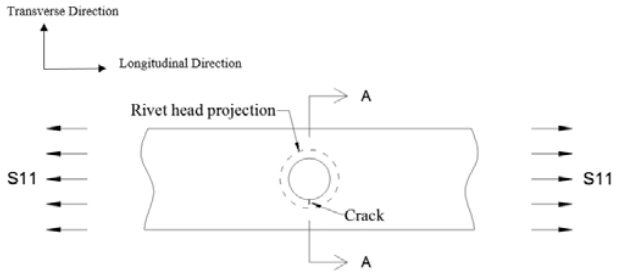


Fig. 8 Crack propagation from a rivet hole due to tensile longitudinal stress

## IV. Summary and Conclusion

A three-dimensional finite element models were developed to obtain the residual stress field generated during a hot-driven riveting process. The model simulates the generation of stress in the material being fastened as the rivet contracts due to a decrease of temperature. These residual stresses play an important role in the fatigue life of the structural components since it induces a localized compressive stress that hinders crack initiation and propagation. Residual stresses were obtained for different cases were the plates being fastened varied in thickness. The beneficial residual stress found in riveted connections decreases as the plate thickness increases. Thus, thicker plates present a lower fatigue life than thinner plates.

Finally, the model was subjected to an external mechanical load to determine the stress field typically encounter near a rivet hole in a steel structural connection typical in older railroad bridges.

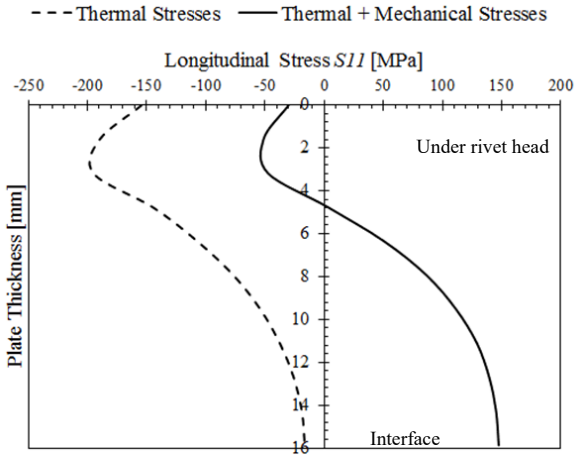


Fig. 9 Thermal and mechanical stresses applied in the riveted model

## APPENDIX

Steel Material Properties

- Yield stress: $\sigma_y = 277.3\text{MPa}$
- Ultimate stress: $\sigma_{ut} = 729.2MPa$
- Density: $\rho = 7850 kg/m^3$
- Volumetric thermal expansion: $\beta = 36x10^{-6}/°C$
- Specific heat capacity, ca, in J/kg °C

$$c_a = 425 + 7.73x10^{-1}T - 1.69x10^{-3}T^2 + 2.22x10^{-6}T^3 \quad 20°C \le T < 600°C$$

$$c_a = 666 + \frac{130002}{T - 738} \quad 600°C \le T < 735°C$$

$$c_a = 545 + \frac{17820}{T - 731} \quad 735°C \le T < 900°C$$

$$c_a = 650 \quad 990°C \le T \le 1200°C$$

- Thermal Conductivity, $\lambda_a$, in W/m·°C

$$\lambda_a = 54 - 3.33x10^{-2}T \quad 20°C \le T < 800°C$$

$$\lambda_a = 27.3 \quad 800°C \le T \le 1200°C$$

- Modulus of elasticity, E, in MPa

$$E = E_o\left(1 + \frac{T}{2000 * Log\left(\frac{T}{1100}\right)}\right) \quad 20°C < T \le 600°C$$

$$E = E_o\left(\frac{690 - 0.69T}{T - 53.5}\right) \quad 600°C < T \le 1000°C$$

where $E_o$ is Young's modulus at 20 °C.

- Poisson's Ratio

$$\upsilon = 3.78x10^{-5}T + 0.283 \quad 0 \le T \le 450°C$$

$$\upsilon = 9.20x10^{-5}T + 0.259 \quad T > 450°C$$

- Interface contact thermal conductance

Steel/air/steel is with a normal grinding surface finish and zero contact pressure.

TABLE I
INTERFACIAL GAP CONDUCTANCE

| Gap (mm) | Thermal Conductance (W/m$^2$°C) |
|---|---|
| 0 | 2500 |
| 0.5 | 50 |
| 1.0 | 25 |
| 1.5 | 0 |

## ACKNOWLEDGMENT

The authors would like to thank the American Association of Railroads and Texas A&M High Performance Research Computing for their continuous support.

## REFERENCES

[1] J. F. Unsworth, "Heavy Axle Load (HAL) Effects on Fatigue Life of Steel Bridges," presented at the TRB 2003 Annual Meeting, 2003.
[2] G. A. Maney, "Clamping force, the Silent Partner in Riveted-Joint Dependability," *Fasteners,* vol. 1, pp. 10-13, 1944.
[3] J. M. M. Out, J. W. Fisher, and B. T. Yen, "Fatigue strength of weathered and deteriorated riveted members, October 1984. (DOT/OST/P-34/85/016) 138p," Fritz Laboratory Reports 2282, 1984.
[4] Y. Zhou, "Fatigue strength evaluation of riveted bridge members," Degree of Doctor of Philosophy in Civil Engineering, Civil Engineering, Lehigh University, Bethlehem, Pennsylvania, 1994.
[5] E. A. Al-Bahkali, "Finite Element Modeling for Thermal Stresses Developed in Riveted and Rivet-Bonded Joints," *International Journal of Engineering & Technology IJET-IJENS,* vol. 11, pp. 86-92, 2011.
[6] A. De Jesus, J. Da Silva, A. Da Silva, and A. Fernandes, "Fatigue Behavior of Riveted and Bolted Connections Made of Puddle Iron - Part II: Numerical Investigation," presented at the 21st Brazilian Congress of Mechanical Engineering, Natal, Brazil, 2011.
[7] Simulia. Abaqus/CAE 6.14 Documentation (Online).
[8] E. C. f. Standardization, "Eurocode 3: Design of steel structures," in *Part 1-2: General Rules - Structural Fire Design*, ed. Brussels, April 2005, pp. 23-26.
[9] J. W. Fisher, G. L. Kulak, and I. F. C. Smith, "A Fatigue Primer for Structural Engineers," N. S. B. Alliance, Ed., ed, 1998.
[10] G. Glinka, "Effect of Residual Stresses on Fatigue Crack Growth in Steel Weldments under Constant and Variable Amplitude Loads," *Fracture Mechanics, ASTM STP 677, American Society for Testing and Materials,* pp. 198-214, 1979.
[11] AREMA, "Manual for Railway Engineering," in *Chapter 15: Steel Structures*, ed, 2015.

**Jackeline Kafie Martinez** is a PhD candidate at Texas A&M University at College Station, Texas. Her dissertation deals with fatigue life of riveted connections in old railroad bridges using a linear elastic fracture mechanics approach. She was born in Honduras, where she got a Bachelor of Science in Civil Engineering. In 2013, she graduated from Texas A&M University with a Master's Degree in Civil Engineering with emphasis in Structures.

**Peter B. Keating** is an Associate Professor at Texas A&M University at College Station, Texas, where he teaches both undergraduate and graduate courses. He holds a PhD degree from Lehigh University. His primary area of research is in structural fatigue with emphasis on steel bridges and petroleum pipelines.